Differential expression profiles of glycosphingolipids in human breast cancer stem cells vs. cancer non-stem cells

Yuh-Jin Liang[a,b,c,1], Yao Ding[a,b,1], Steven B. Levery[d], Marlin Lobaton[a], Kazuko Handa[a], and Sen-itiroh Hakomori[a,b,2]

[a]Division of Biomembrane Research, Pacific Northwest Research Institute, Seattle, WA 98122; [b]Departments of Pathobiology and Global Health, University of Washington, Seattle, WA 98195; [c]Chang Gung Memorial Hospital at Linkou, Taoyuan 333, Taiwan; and [d]Copenhagen Center for Glycomics and Department of Cellular and Molecular Medicine, University of Copenhagen, 2200 Copenhagen, Denmark

Contributed by Sen-itiroh Hakomori, February 13, 2013 (sent for review December 5, 2012)

Previous studies demonstrated that certain glycosphingolipids (GSLs) are involved in various cell functions, such as cell growth and motility. Recent studies showed changes in GSL expression during differentiation of human embryonic stem cells; however, little is known about expression profiles of GSLs in cancer stem cells (CSCs). CSCs are a small subpopulation in cancer and are proposed as cancer-initiating cells, have been shown to be resistant to numerous chemotherapies, and may cause cancer recurrence. Here, we analyzed GSLs expressed in human breast CSCs by applying a CSC model induced through epithelial–mesenchymal transition, using mass spectrometry, TLC immunostaining, and cell staining. We found that (*i*) Fuc-(n)Lc4Cer and Gb3Cer were drastically reduced in CSCs, whereas GD2, GD3, GM2, and GD1a were greatly increased in CSCs; (*ii*) among various glycosyltransferases tested, mRNA levels for ST3GAL5, B4GALNT1, ST8SIA1, and ST3GAL2 were increased in CSCs, which could explain the increased expression of GD3, GD2, GM2, and GD1a in CSCs; (*iii*) the majority of GD2+ cells and GD3+ cells were detected in the $CD44^{hi}/CD24^{lo}$ cell population; and (*iv*) knockdown of ST8SIA1 and B4GALNT1 significantly reduced the expression of GD2 and GD3 and caused a phenotype change from CSC to a non-CSC, which was detected by reduced mammosphere formation and cell motility. Our results provide insight into GSL profiles in human breast CSCs, indicate a functional role of GD2 and GD3 in CSCs, and suggest a possible novel approach in targeting human breast CSCs to interfere with cancer recurrence.

Extensive studies have illustrated aberrant glycosylation in cancer cells (reviewed in refs. 1 and 2). Glycosylation changes associated with oncogenic transformation have been studied, initially focusing on glycosphingolipids (GSLs)*, particularly on the reduction of monosialoganglioside GM3 (5) or other gangliosides (6) along with an increase of the precursor GSLs (5–8). Certain gangliosides inhibited the growth factor-induced activation of tumor phenotype through the inhibition of receptor-associated tyrosine kinases (7). Subsequent studies indicated that this process was assumed to be based on binding of specific gangliosides to the extracellular domain of epidermal growth factor receptor (8). The studies of *N*- or *O*-linked glycosylations (9, 10) and their biosynthetic pathways were well reviewed in a monograph edited by W. J. Lennarz (11).

Since the cloning of the glycosyltransferases (GTs) gene was initiated with β1-4Gal transferase in 1986 (12, 13), as many as ~180 genes have been cloned so far. GTs genes have applied to various studies, particularly molecular mechanisms of cancer progression. GM3 was found to be reduced in v-Jun-induced transformed cells, and the transfection of the GM3 synthase gene caused reversion from oncogenic to normal-type cells, whereby GM3–CD9 (Tetraspanin-29) complex was restored in the membrane microdomain, as observed in normal cells (14). The FucTIII gene which encode alpha (1,3/1,4)fucosyltransferase was shown to cause tumor cell metastasis via expression of Sialyl Lewis A (SLe^a), which binds to E-selectin (15), and enhanced synthesis of mucin type-3 core, by activation of β3GlcNAc transferase, induced the inhibition of metastasis in colon cancer through reducing the mucin type-1 core, Galβ3GalNAc (16).

Since the epithelial–mesenchymal transition (EMT) process was proposed in embryonic development (17, 18), many studies reported its involvement in diseases, particularly in cancer progression (19–21). The involvement of glycosylation in the EMT process was unclear, particularly in GSLs. Recently, specific GSLs were found to down-regulate during EMT, and enhanced expression of the GSLs blocked the EMT process (22, 23).

The process of embryonal development from a fertilized egg to blastocysts was closely associated with a clear change in glycosylation from globo to lacto to ganglio structures (24). Recent studies indicated a drastic change in GSL expression during differentiation of human embryonic stem cells into various cell lineages (25, 26). Here, we report a series of GSL expression profiles in cancer stem cell (CSC) vs. non-CSC populations using human mammary cell lines.

There is growing evidence for the existence of CSCs, which are a small subset of cells within a tumor, capable of self-renewing and initiating/sustaining tumor growth (reviewed in ref. 27). CSCs have been identified and characterized in numerous human malignancies: $CD34^+CD38^{lo}$ in acute myeloid leukemias, $CD133^+$ in brain tumors, $CD166^+$ in gastric cancers, $EpCAM^+$ in hepatomas, and $CD44^{hi}CD24^{lo}$ in breast tumors. All of these phenotypes were shown to be associated with tumor initiation and metastasis, and these cell-surface molecules were described as CSC markers (28–32). In addition, it has been indicated that CSCs are resistant to various chemo- and radiotherapies and can cause cancer relapse and metastasis (33–37). Therefore, great efforts are being made to identify a unique CSC phenotype, to better identify and target CSCs.

Following the original study of Al Hajj et al. (31), many studies implicated $CD44^{hi}/CD24^{lo}$ as a CSC marker for breast cancer, because $CD44^{hi}/CD24^{lo}$ cells showed high tumorigenicity in xenograft assays, enhanced invasiveness, and enhanced mammosphere formation. In addition, the cells share some common features with normal stem cells, such as the abilities to self-renew and generate heterogeneous progeny (38, 39). Moreover, Ricardo et al. (40) reported that there was a higher frequency of $CD44^{hi}/CD24^{lo}$ in more aggressive basal-like breast tumors than in less-aggressive luminal breast cancers; together with this, a mathematical model showed that the abundance of $CD44^{hi}/CD24^{lo}$ correlates positively with tumor aggressiveness (41).

Accumulating evidence supports the idea that aberrant activation of EMT, a latent embryonic program, can increase the ability

Author contributions: Y.-J.L., S.B.L., K.H., and S.H. designed research; Y.-J.L., Y.D., S.B.L., and M.L. performed research; S.B.L. contributed new reagents/analytic tools; Y.-J.L., Y.D., S.B.L., K.H., and S.H. analyzed data; and Y.-J.L., Y.D., S.B.L., K.H., and S.H. wrote the paper.

The authors declare no conflict of interest.

[1]Y.-J.L. and Y.D. contributed equally to this work.

[2]To whom correspondence should be addressed. E-mail: hakomori@u.washington.edu.

This article contains supporting information online at www.pnas.org/lookup/suppl/doi:10.1073/pnas.1302825110/-/DCSupplemental.

*The nomenclature for glycosphingolipids follows the International Union of Pure and Applied Chemistry and International Union of Biochemistry recommendations (3) and the system of Svennerholm (4).

of cancer cells to migrate and invade and is linked with metastatic ability (42, 43). It was also reported that EMT induction in immortalized human mammary epithelial cells increased the $CD44^{hi}CD24^{lo}$ population and tumor-sphere formation (44, 45).

The CSC population is a very minor subset of cells in tumors, only ~1% in colon cancer and leukemia and ~2% in breast cancer (46–48); therefore, it is necessary to enrich CSCs to study the possible role of GSLs therein. Recently, an in vitro EMT model, the immortalized human mammary epithelial cell (HMLE)-Twist-ER, was established (42). Upon the induction of Twist expression by tamoxifen, the epithelial cells developed a mesenchymal morphology and acquired CSC properties (44, 49). We adopted the model and assessed the different expression profiles of GSLs in CSCs compared with non-CSCs.

In this study, we used electrospray ionization (ESI)-MS, high-performance TLC (HPTLC), in situ cell staining, and flow cytometry to characterize changes in GSL expression. Our results suggest that GD3 and GD2 may play a functional role in maintaining the CSC phenotype in human breast cancer.

Results

Changes of GSL Profiles Between CSCs and Non-CSCs. To study the difference in GSL expression between CSCs and non-CSCs in human breast cancer, we used the HMLE-Twist-ER cell system developed and used by Weinberg's group for their own studies on CSCs (20, 34). HMLE-Twist-ER cells expressed the EMT transcription factor Twist in an estrogen receptor (ER)-based inducible system. Culturing the cells in the presence of tamoxifen, an ER ligand, for about 10 d induced the expression of Twist, resulting in a change in the EMT and cell morphology from epithelial to fibroblast-like mesenchymal type (Fig. S1*A*). Along with morphological changes, the mRNA expression profile changed from an epithelial type to a mesenchymal type. Furthermore, cell motility activity, measured by phagokinetics assay, increased, and the stem cell population, as defined by the $CD44^{hi}/CD24^{lo}$ phenotype, also increased (Fig. S1 *A–D*). These observations are in accordance with previous reports (20, 35); therefore, we compared GSL expression profiles in the HMLE-Twist-ER cells and in HMLE-Twist-ER cells cultured in the presence of tamoxifen as breast non-CSCs and CSCs, respectively.

To compare the GSL profile of non-CSCs with CSCs, total GSLs were extracted and separated into a polar upper phase and nonpolar lower phase by Folch partition. Non-GSL impurities, such as phospholipids, sphingomyelin, and plasmalogens in the lower phase were removed by an acetylation method as previously described (36). Purified GSLs from the upper or lower phases were analyzed by Orbitrap-Fourier transform (FT) MS. MS1 results from the Folch partition upper phase GSLs are shown in Fig. 1. Identities of GSLs in MS1 profiles were tentatively assigned based on *m/z* value for major molecular ion signals, fitted to permutations of hexose, N-acetylhexosamine, deoxyhexose, and N-acetylneuraminic acid residues (Hex, HexNAc, deoxyHex, and NeuAc, respectively), in combination with typical sphingosine and fatty acyl components of common ceramides. Confirmations of monosaccharide and ceramide composition were provided by collision-induced dissociation (CID)-MS2 of selected molecular ion precursors. The structures were inferred where possible from knowledge of human GSL expression patterns (for example, a GSL detected with the formula Hex(3)Cer is consistent with the known human GSL globotriaosylceramide, Gb3Cer). A list of all GSL species detected, with their measured and calculated *m/z* values, can be found in Table S1.

Comparing the lower *m/z* segments (Fig. 1 *A* and *B*), it seems that the signal with formula Hex_3-Cer (*m/z* 1,046.6772), which most likely corresponds to Gb3Cer in the control sample, is absent in the CSC sample. In addition, the expression of Fuc-(n)Lc4Cer (*m/z* 1,395.8237, Fig. 1*A*) is significantly reduced in the CSC sample (Fig. 1*B*). This result is consistent with the HPTLC result for the lower phases of the Folch partition (Fig. 2*C Left*) and points to a significantly reduced neutral GSL synthesis in

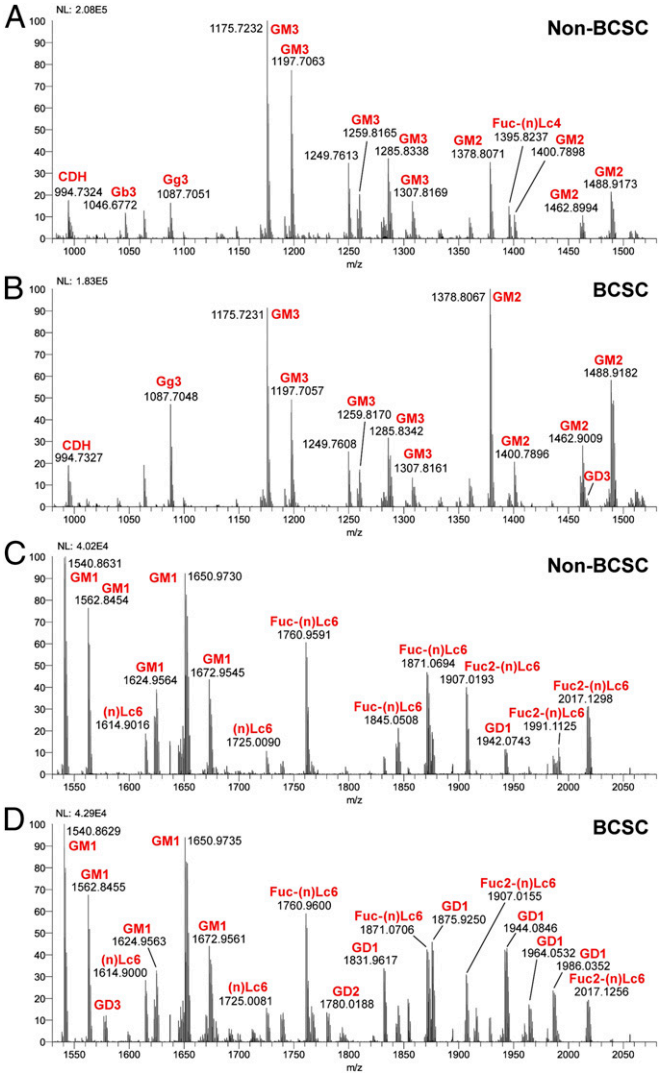

Fig. 1. ESI-MS molecular ion profiles of GSLs from non-CSCs and CSCs. Full spectrums for non-CSCs and CSCs were separated into two groups, *m/z* 980–1,530 and *m/z* 1,530–2,080 as indicated. (*A–D*) Annotations of GSLs on the spectrum were assigned based on *m/z* values typical for ceramide moiety-associated fatty acyl heterogeneity. We deduced that GSLs with the same glycan moiety but different fatty acyl components are the same GSL. NL represents a measure of absolute spectral counts for the most abundant peak (100% on the *y*-axis) in respective segments.

CSC. The down-regulation of Gb3Cer was also confirmed by HPTLC immunostaining (Fig. 2*C Right*). Furthermore, we detected somewhat less GM3 (Fig. 1 *A* vs. *B*) but significantly more GM2, GD3 (Fig. 1 *A* vs. *B*), and GD2 (Fig. 1 *C* vs. *D*) in the CSC sample. The signal corresponding to formula $HexNAc_1Hex_2Cer$ (*m/z* 1,087.7051, Fig. 1*A*) was also increased in the CSC; this signal likely corresponds to gangliotriaosylceramide (Gg3Cer), but it could also arise from partial in-source desialylation of GM2. In the higher *m/z* range, we observed a substantial increase of GD1 in CSCs (Fig. 1 *C* vs. *D*); these results were also consistent with HPTLC results (Fig. 2*B*). Because such a notable difference in the level of GD1 was observed between the two cell types, we performed CID-MS2 on the peaks at *m/z* 1,831 and 1,853. The fragmentation seemed to be consistent with that of GD1a (Fig. S2*A*, CID-MS2 of *m/z* 1,831). Additional CID-MS2 analyses of each of the major precursors in the MS1 spectra were performed; two exemplary MS2 spectra, of Fuc-(n)Lc6Cer and Fuc2-(n)Lc6Cer molecular species, are reproduced in Fig. S2 *B*

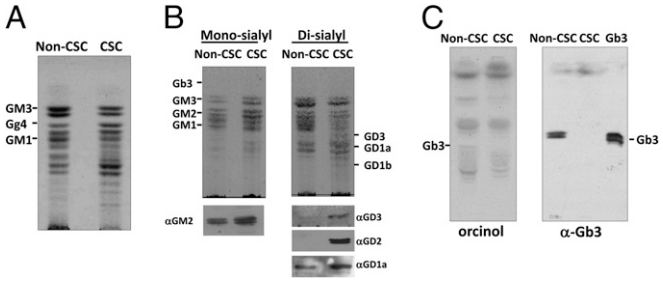

Fig. 2. HPTLC profiles of GSLs extracted from non-CSCs and CSCs. (*A*) Upper-phase GSLs from 5×10^6 non-CSCs and CSCs were separated on an HPTLC plate and visualized by orcinol spraying. (*B*) Monosialoganglioside (Mono-sialyl) GSL or disialoganglioside (Di-sialyl) GSL fractions were separated from total polar upper-phase GSLs with DEAE-Sephadex columns. GSLs were visualized by orcinol spraying and characterized by immunostaining with mAbs specific to GM2, GD3, GD2, or GD1a. (*C*) Lower-phase GSLs from 5×10^6 non-CSCs and CSCs were processed for the detection by orcinol spraying or immunostaining with anti-Gb3Cer mAb.

and *C*, respectively. In summary, by using ESI-MS profiling, we found Gb3Cer and Fuc-(n)Lc4Cer were down-regulated in CSCs and that simultaneously GM2, GD3, GD2, and GD1 were significantly up-regulated in CSCs.

Analysis of the Changes of GSL Expression Profiles by HPTLC Immunostaining and Immunofluorescence Cell Staining. MS results for the expression of GSLs in non-CSC and CSC samples were confirmed by HPTLC immunostaining. GSLs in the upper phase were fractionated into upper-neutral, monosialogangliosides, disialogangliosides, trisialogangliosies, and polysialogangliosides with a DEAE-Sephadex column as described in *Materials and Methods*. GSLs developed on TLC plates were stained with orcinol/sulfuric acid or detected by immunostaining with specific mAbs (Fig. 2). As shown in Fig. 2*A*, the total upper-phase GSLs from the two cell populations exhibited different orcinol staining patterns. Up-regulation of GM2, GD2, GD3, and GD1a in CSCs was confirmed with TLC immunostaining using fractions isolated with DEAE-Sephadex. Gb3Cer was analyzed using fractions from both the upper and lower phases. As expected, the upper-phase fraction did not exhibit any detectable amount of Gb3Cer in either CSCs or non-CSCs, whereas the lower-phase fraction showed clear down-regulation of Gb3Cer in CSCs (Fig. 2*C*). The results for GM2, GD2, GD3, GD1a, and Gb3Cer were consistent with MS data. We further analyzed GSL localization via in situ cell staining. As shown in Fig. S3, GM2, GD2, GD3, and GD1a were expressed on the cell surface and up-regulated in CSCs; however, the signals for Gb3Cer were localized inside the cells. In addition, the signals for Gb3Cer were not significantly different between non-CSCs and CSCs (Fig. S3). Different Gb3Cer expression levels detected by MS and HPTLC immunostaining were not observed by cell staining. This is most probably due to cross-reactivity of the anti-Gb3 antibody.

Expression Levels of mRNAs for GSL Synthases Detected by Real-Time RT-PCR. To identify GTs responsible for the different expression of GSLs in non-CSCs and CSCs, mRNA levels for several GT candidates were determined by real-time RT-PCR. To ensure the results from the real-time RT-PCR analyses were reliable, we optimized the amount of cDNA and kept the threshold cycle (Ct) values of the target genes less than 35. As shown in Fig. 3*A*, the expression level of GM3 synthase (ST3GAL5, which encode ST3 beta-galactoside alpha-2,3-sialyltransferase 5), GM2/GD2 synthase (B4GALNT1, which encode beta-1,4-N-acetyl-galactosaminyl transferase 1), GD3 synthase (ST8SIA1, which encode ST8 alpha-N-acetyl-neuraminide alpha-2,8-sialyltransferase 1), and GD1a synthase (ST3GAL2, which encode ST3 beta-galactoside alpha-2,3-sialyltransferase 2) in CSCs increased 8.2-, 5.0-, 90.6-, and 8.1-fold, respectively, explaining the up-regulation of GD3, GD2, GM2, and GD1a in CSCs. It is noted that in the experiments Ct values for β-actin were 14–15, whereas Ct values for the ST8SIA1 gene were 33–34 and 26–27 in non-CSC and in CSC, respectively. However, the expression of A4GALT, FUT1, and FUT4 candidates for GTs responsible for Gb3Cer (globo-series GSLs) and Fuc-(n)Lc4Cer [(n)lacto-series GSLs] expression did not show any significant difference between CSCs and non-CSCs (Fig. 3 *B* and *C*). Furthermore, the expression of Gb3Cer-related glycosidases, α-galactosidase (GAL), and hexosaminidase (Hexa-B) also remain constant between non-CSCs and CSCs. Therefore, the mRNA levels could not explain the loss of Gb3Cer in CSCs (Fig. 3*B*). The fold changes of GT gene expression are summarized and shown along with ganglio-series, globo-series, and

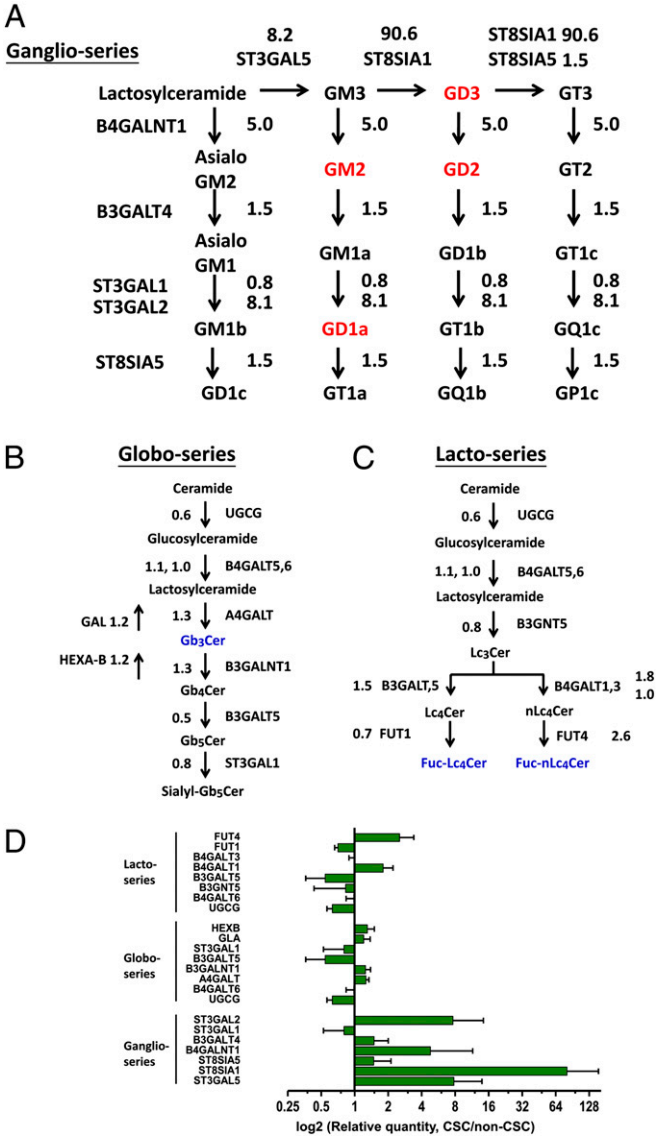

Fig. 3. Changes in mRNA levels of GTs between non-CSCs and CSCs. GTs involved in the synthesis of (*A*) ganglio-series GSLs, (*B*) globo-series GSLs, and (*C*) lacto- or neolacto-series GSLs are shown. The expression levels of GT genes were analyzed and quantified by real-time RT-PCR. GSLs up-regulated in CSCs are distinguished in red. GSLs down-regulated in CSCs are distinguished in blue. Diagram quantities represent the ratio of expression of CSCs to non-CSCs. (*D*) Fold changes of GT gene expression between non-CSCs and CSCs were summarized. Values on the *y*-axis represent log2 relative quantities. Data represent the mean of three independent experiments. Error bars represent 1 SD from the mean of relative quantities.

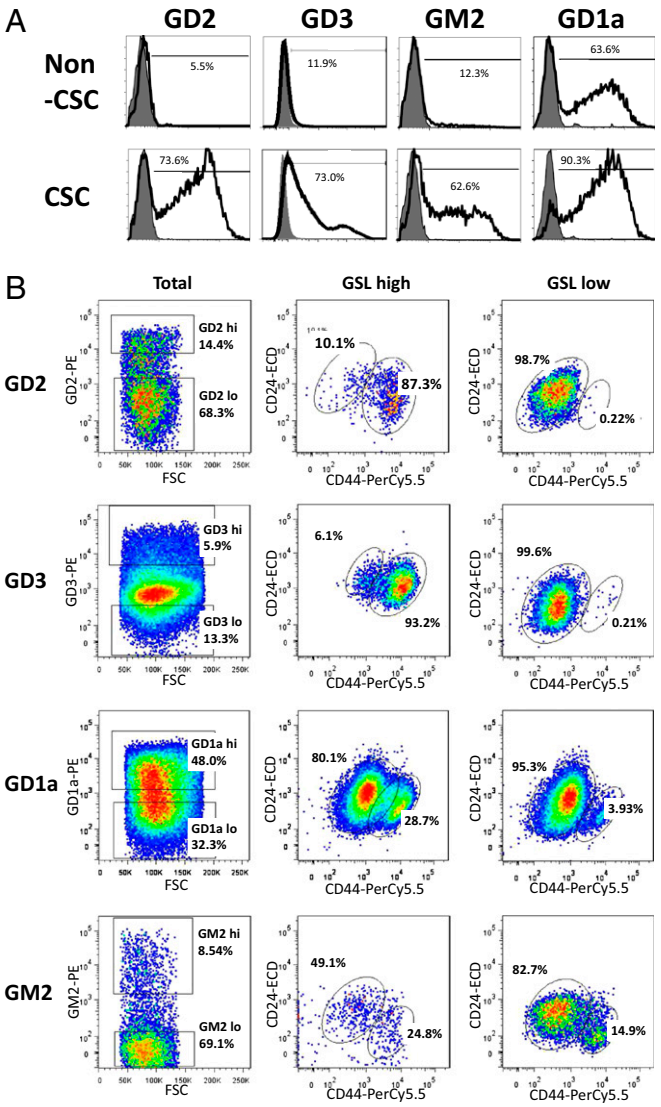

Fig. 4. Correlation of the expression levels of the GSLs with the $CD44^{hi}/CD24^{lo}$ phenotype. (*A*) The expressions of GSLs in CSCs and non-CSCs were analyzed by flow cytometry. Up-regulation of GD2, GD3, GM2, and GD1a in CSCs were detected with flow cytometry. Cells were stained with antibodies against indicated GSLs and are shown with solid line. Stained isotype controls are shown in gray. Values presented the mean of three experiments. (*B*) HMLE-Twist-ER cells were triple-stained with anti–CD44-PC5, anti–CD24-ECD, and GSL-specific antibodies conjugated with phycoerythrin then analyzed by flow cytometry. Plots are gated for GSL-high or GSL-low populations in plots labeled "Total." Plots are gated for $CD44^{hi}$ and $CD24^{lo}$ in plots labeled "GSL high" and "GSL low."

(n)lacto-series GSL biosynthesis pathways in Fig. 3 *A*–*D*. Following these results, we focused on ST3GAL5, B4GALNT1, and ST8SIA1, hypothesizing that the GTs explain the differential expression of GD2, GD3, GM2, and GD1a between non-CSCs and CSCs.

Correlation Between GSL Expression and the $CD44^{hi}/CD24^{lo}$ Profile. First, we analyzed the expression of GD2, GD3, GD1a, and GM2 by flow cytometry. Consistent with the results from MS, TLC, and cell staining (Figs. 1 and 2 and Fig. S3), flow cytometry analysis demonstrated that GD2, GD3, GD1a, and GM2 expression were much higher in CSCs than in non-CSCs (Fig. 4*A*).

Next, we examined the correlation between the expression level of the GSLs and the $CD44^{hi}/CD24^{lo}$ profile, one of the characteristic features of human breast CSCs. HMLE-Twist-ER cells treated with tamoxifen for 5 d (for partial EMT induction) were stained with Fluor-conjugated antibodies against CD44 (anti–CD44-PerCP-Cy5.5), CD24 (anti–CD24-ECD), and GSLs (anti–GD2-PE, anti–GD3-PE, anti–GD1a-PE, or anti–GM2-PE). The results of the triple-color analysis indicated that more than 87% of the $GD2^{hi}$ cell population exhibited a $CD44^{hi}/CD24^{lo}$ profile, but only 0.2% of the $GD2^{lo}$ cell population (Fig. 4*B*, GD2 panel). Additionally, we found that more than 93% of the $GD3^{hi}$ population exhibited a $CD44^{hi}/CD24^{lo}$ CSC profile, but only 0.2% of the $GD3^{lo}$ population (Fig. 4*B*, GD3 panel). By contrast, GD1a and GM2 are not capable of independently enriching for CSCs (Fig. 4*B*, GD1a panel). $GD1a^{hi}$ and $GD1a^{lo}$ cell populations exhibited similar CD44/CD24 profiles (Fig. 4*B*, GD1a panel). There were also no clear contrast CD44/CD24 profiles between $GM2^{hi}$ or $GM2^{lo}$ cell population (Fig. 4*B*, GM2 panel). These results indicate that the expression of GD2 and GD3 are correlated more strongly with the $CD44^{hi}/CD24^{lo}$ CSC profile than that of GD1a and GM2 (Fig. 4*B*).

Functional Role of GD2 and GD3 in CSCs. Based on the above results, we analyzed the functional role of GD2 and GD3 and the involved GTs for their biosynthesis, B4GALNT1 and ST8SIA1, which were also up-regulated in CSCs. The human breast cancer cell line MCF7, which was reported to contain a subpopulation $CD44^{hi}CD24^{lo}$ cells with features of stem cells (50, 51) and expressed GD2 and GD3 at a satisfactory level as shown in this study, was used in knockdown experiments with a lentiviral-based shRNA expression vector, because it was difficult to transfect HMLE-Twist-ER cells efficiently enough for functional assays, mammosphere formation, and cell motility activity. At the mRNA level, we observed 82% and 51% suppression for ST8SIA1 and B4GALNT1, respectively (Fig. 5*A*). As expected, ST8SIA1 knockdown reduced 27% of $GD2^{+}$ and 60% of $GD3^{+}$ cells, whereas the B4GALNT1 knockdown only reduced 38% of $GD2^{+}$ cells and did not change the percentage of $GD3^{+}$ cells (Fig. 5*B*).

Reversion of CSC phenotype to non-CSC phenotype in the ST8SIA1 and B4GALNT1 knockdown cells were evaluated with two characteristic features of human breast CSC: mammosphere formation efficiency and cell motility activity. Mammospheres are floating spherical colonies driven from a small population of human breast cancer cells that are capable of survival and proliferation under anchorage-independent conditions in vitro (52). It has been shown that the cells forming mammospheres have CSC properties based on their ability to self-renew, initiate, and/or sustain heterogeneous tumors (53). ST8SIA1 knockdown cells (ST8SIA1-KD) and B4GALNT1 knockdown cells (B4GALNT1-KD) formed fivefold fewer (22% of control) and twofold fewer (50% of control) mammospheres than control mock cells, respectively (Fig. 5*C*). Cell motility activity, which was assessed by phagokinetic motility assay, demonstrated that the migration areas of ST8SIA1-KD and B4GALNT1-KD cells were only 8% and 18% of those of the control cells, respectively (Fig. S4). The findings indicate that GD2 and GD3, together with associated GTs ST8SIA1 and B4GALNT1, play a functional role in human breast CSCs.

Discussion

In this study, we compared GSL expression in CSCs and non-CSCs using a human mammary cell line that was extensively studied as a breast CSC model (44). We observed that Gb3Cer expression is diminished and that Fuc-(n)Lc4Cer expression is decreased in CSCs. Conversely, GD3, GD2, GM2, and GD1a were up-regulated, and mRNA levels of the GTs ST3GAL5, ST8SIA1, B4GALNT1, and ST3GAL2 were also up-regulated. Moreover, the number of GD3- and GD2-expressing cells were higher in the $CD44^{hi}/CD24^{lo}$ population. Knockdown of GD3/GD2-associated GTs, ST8SIA1 and B4GALNT1, significantly reduced mammosphere formation and inhibited cell motility.

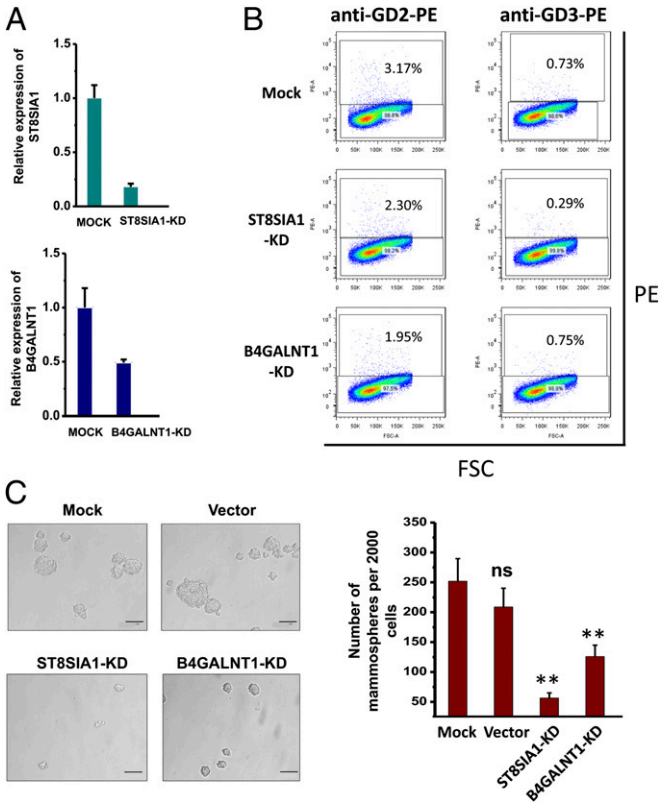

Fig. 5. Knockdown of ST8SIA1, B4GALNT1, or ST3GAL5 reduces mammosphere formation in MCF-7 cells. (*A*) Real-time RT-PCR illustrates a reduction in mRNA levels after transfection of shRNA against ST8SIA1 or B4GALNT1. Relative expressions for target genes are shown on the *y*-axis. (*B*) Expression of GD2 or GD3 decreased after knockdown of ST8SIA1 and B4GALNT1. GD2 or GD3 expression (*y*-axis) and forward scatter (FSC) (*x*-axis) are shown. Percentages represent GSL-positive cells plots. (*C*) Mammosphere formation of mock control, vector control, ST8SIA1-KD, or B4GALNT1-KD cells. Microscope magnification was ×200. Data represent the mean of three independent experiments. ns, not significant; $^{**}P \leq 0.005$. (Scale bar, 0.1 mm.)

Our data indicate that both GD2 and GD3 could be new markers for breast CSCs and also function to maintain CSC properties.

In the case of Gb3Cer, its depletion in CSCs was detected by both MS and TLC immunostaining (Figs. 1*A* and 2*C*), but mRNA levels of GTs A4GALT and B3GALNT1 and glycosidases GAL and Hexa-B, which were analyzed as possibly responsible enzymes for the Gb3Cer depletion, did not show significant difference (Fig. 3*B*). One possible explanation might be that GM3 synthase (ST3GAL5), which was up-regulated by 8.2-fold in CSCs (Fig. 3*A*), competes with Gb3 synthase for the common precursor lactosylceramide (LacCer) and results in depletion of Gb3Cer expression. An alternative explanation might be, as recently reported for transmembrane BAX inhibitor motif containing (TMBIM) family genes (54), the reduction of Gb3Cer expression without changing the mRNA of Gb3 synthase by post-transcriptional regulation. Thus, the possible mechanism for the depletion of Gb3Cer in CSCs and its possible functional role in CSCs remain to be studied.

CD44 and CD24 have been used extensively in combination with other markers to isolate CSCs from solid tumors. The present study on the correlation between the expression of GD3, GD2, GM2, or GD1a with the CD44/CD24 marker in CSCs demonstrated that the expression of GD3 and GD2 was higher in the $CD44^{hi}/CD24^{lo}$ population, although GM2 and GD1a did not correlate well with the $CD44^{hi}/CD24^{lo}$ profile (Fig. 4*B*). In addition to $CD44^{hi}/CD24^{lo}$, aldehyde dehydrogenase 1 (ALDH1), CD133, CD29 (β1-integrin), CD49f (α6-integrin), and CD61 (β3-integrin) were reported as markers of breast CSCs (reviewed in ref. 55). Future studies will clarify whether GM2 and GD1a expression is correlated with these stem cell markers.

A recent study by Andreeff and coworkers (56) reported enhanced expression of GD2 in a human breast CSC population. They showed that the suppression of GD3 synthase, ST8SIA1, abrogated tumor formation completely. In this present study, we found that not only GD2 but also GD3 are expressed predominantly in the $CD44^{hi}/CD24^{lo}$ population. In addition to the knockdown of ST8SIA1, which reduced both GD2 and GD3, the knockdown of B4GALNT1, which reduced only GD3, also resulted in a significant reduction in mammosphere formation and cell motility, suggesting functional roles of GD3 in addition to GD2 in CSCs. Aside from the present study, GD3 was reported to be overexpressed in melanoma, hepatoma, and ovarian cancer and to inhibit natural killer T-cell activation and suppress the innate immune response in ovarian cancer (57). GD2 has been found to be overexpressed in neuroblastoma and melanoma, and targeting GD2 by a vaccine approach was developed for these cancers (58). In osteosarcoma, GD2/GD3-expressing cells were shown to enhance malignancy (59). These data support our present results that GD2 and GD3 are cancer-associated antigens, especially CSC-associated epitopes, and are promising candidates for cancer therapy (60).

Aberrant expression of carbohydrate structures in cancer, including GSLs, has been known for decades (61, 62), and GSLs in tumor cells have been shown to change their structure and organization in the membrane to promote tumor progression (60). In addition to GSLs indicated to be associated with CSCs in this study, the following were found to be highly expressed in human cancer but either absent or present in negligible amounts in normal cells/tissues: (*i*) blood group A-like antigens expressed in tumor cells of blood group O or B patients [the structure is GalNAcα1-O-Ser/Thr, termed Tn (63–65]; (*ii*) sialyl 2-6Tn antigen [i.e., NeuAcα2-6GalNAcα1-O-Ser/Thr (66)]; and (*iii*) extended type-I antigen [i.e., Le^a on Le^a (67) or Le^b on Le^a (68, 69)]. Whether these glycan structures are somehow associated with CSCs is an interesting point for future studies.

Materials and Methods

The full materials and methods are provided in *SI Materials and Methods*.

Mass Spectrometry. GSLs were analyzed by electrospray ionization–linear ion trap–Orbitrap–Fourier transform–mass spectrometry (ESI-LIT-Orbitrap-FT-MS) in an LTQ-Orbitrap XL hybrid instrument (Thermo-Scientific) operated in the positive ion mode. Samples were dissolved in pure methanol and introduced by direct infusion via a TriVersa NanoMate ESI-Chip interface (Advion BioSystems) at a flow rate of ~100 nL/min. The NanoMate spray voltage was kept at 1.5 kV. Spray current was generally in the range of 50–150 nA. For CID-MS2 analyses, the following parameters were used: precursor isolation width, *m/z* 5.0; normalized collision energy, 35 V; activation Q, 0.250; activation time, 30 ms. All spectra were acquired in Orbitrap-FT mode (30,000 nominal resolution), accumulated for 1 min in the case of MS1 and 0.5 min in the case of CID-MS2. All precursor and fragment ions were detected as sodium adducts.

Knockdown of B4GALNT1 and ST8SIA1. Plasmids containing B4GALNT1 shRNA (RHS3979-9603789) and ST8SIA1 shRNA (RHS3979-9603453) or empty vector (PLKO.1) were purchased from Open Biosystems. Plasmids were purified and transfected into MCF-7 cells using Lipofectamine LTX & Plus Reagent (Invitrogen). After 72 h of transfection, cells were split and selected with puromycin at 0.5 μg/mL Puromycin-resistant colonies were screened for mRNA levels corresponding to each glycosyltransferase by real-time RT-PCR.

ACKNOWLEDGMENTS. We thank Dr. Robert A. Weinberg for providing the HMLE-Twist-ER cell line, Will Price for technical assistance, Dave Osborn (BeckmanCoulter) for flowcytometry technical support, and Malcolm Gilbert and Dr. Wai Cheu Lai for the preparation of the manuscript. S.B.L. is funded by a Danish National Research Foundation Center of Excellence grant to the Copenhagen Center for Glycomics (DNRF107). This study was supported by the Biomembrane Institute.

1. Handa K, Hakomori SI (2012) Carbohydrate to carbohydrate interaction in development process and cancer progression. *Glycoconj J* 29(8-9):627–637.
2. Hakomori SI (2010) Glycosynaptic microdomains controlling tumor cell phenotype through alteration of cell growth, adhesion, and motility. *FEBS Lett* 584(9):1901–1906.
3. International Union of Pure and Applied Chemistry and International Union of Biochemistry Commission on Biochemical Nomenclature (1977) The nomenclature of lipids. Recommendations 1976. *Lipids* 12(6):455–468.
4. Svennerholm L (1964) The Gangliosides. *J Lipid Res* 5:145–155.
5. Hakomori SI, Murakami WT (1968) Glycolipids of hamster fibroblasts and derived malignant-transformed cell lines. *Proc Natl Acad Sci USA* 59(1):254–261.
6. Mora PT, Brady RO, Bradley RM, McFarland VW (1969) Gangliosides in DNA virus-transformed and spontaneously transformed tumorigenic mouse cell lines. *Proc Natl Acad Sci USA* 63(4):1290–1296.
7. Miljan EA, Bremer EG (2002) Regulation of growth factor receptors by gangliosides. *Sci STKE* 160:re15.
8. Miljan EA, et al. (2002) Interaction of the extracellular domain of the epidermal growth factor receptor with gangliosides. *J Biol Chem* 277(12):10108–10113.
9. Buck CA, Glick MC, Warren L (1971) Effect of growth on the glycoproteins from the surface of control and Rous sarcoma virus transformed hamster cells. *Biochemistry* 10(11):2176–2180.
10. Ogata SI, Muramatsu T, Kobata A (1976) New structural characteristic of the large glycopeptides from transformed cells. *Nature* 259(5544):580–582.
11. Lennarz WJ (1980) *The Biochemistry of Glycoproteins and Proteoglycans* (Plenum, New York).
12. Narimatsu H, Sinha S, Brew K, Okayama H, Qasba PK (1986) Cloning and sequencing of cDNA of bovine N-acetylglucosamine (beta 1-4)galactosyltransferase. *Proc Natl Acad Sci USA* 83(13):4720–4724.
13. Shaper NL, et al. (1986) The human galactosyltransferase gene is on chromosome 9 at band p13. *Somat Cell Mol Genet* 12(6):633–636.
14. Miura Y, et al. (2004) Reversion of the Jun-induced oncogenic phenotype by enhanced synthesis of sialosyllactosylceramide (GM3 ganglioside). *Proc Natl Acad Sci USA* 101(46):16204–16209.
15. Nishihara S, et al. (1994) Molecular genetic analysis of the human Lewis histo-blood group system. *J Biol Chem* 269(46):29271–29278.
16. Iwai T, et al. (2005) Core 3 synthase is down-regulated in colon carcinoma and profoundly suppresses the metastatic potential of carcinoma cells. *Proc Natl Acad Sci USA* 102(12):4572–4577.
17. Sugrue SP, Hay ED (1981) Response of basal epithelial cell surface and cytoskeleton to solubilized extracellular matrix molecules. *J Cell Biol* 91(1):45–54.
18. Greenburg G, Hay ED (1982) Epithelia suspended in collagen gels can lose polarity and express characteristics of migrating mesenchymal cells. *J Cell Biol* 95(1):333–339.
19. Hay ED (2005) The mesenchymal cell, its role in the embryo, and the remarkable signaling mechanisms that create it. *Dev Dyn* 233(3):706–720.
20. Turley EA, Veiseh M, Radisky DC, Bissell MJ (2008) Mechanisms of disease: Epithelial-mesenchymal transition—Does cellular plasticity fuel neoplastic progression? *Nat Clin Pract Oncol* 5(5):280–290.
21. Thiery JP, Acloque H, Huang RY, Nieto MA (2009) Epithelial-mesenchymal transitions in development and disease. *Cell* 139(5):871–890.
22. Guan F, Handa K, Hakomori SI (2009) Specific glycosphingolipids mediate epithelial-to-mesenchymal transition of human and mouse epithelial cell lines. *Proc Natl Acad Sci USA* 106(18):7461–7466.
23. Guan F, Schaffer L, Handa K, Hakomori SI (2010) Functional role of gangliotetraosylceramide in epithelial-to-mesenchymal transition process induced by hypoxia and by TGF-beta. *FASEB J* 24(12):4889–4903.
24. Fenderson BA, Andrews PW, Nudelman E, Clausen H, Hakomori SI (1987) Glycolipid core structure switching from globo- to lacto- and ganglio-series during retinoic acid-induced differentiation of TERA-2-derived human embryonal carcinoma cells. *Dev Biol* 122(1):21–34.
25. Liang YJ, et al. (2011) Changes in glycosphingolipid composition during differentiation of human embryonic stem cells to ectodermal or endodermal lineages. *Stem Cells* 29(12):1995–2004.
26. Liang YJ, et al. (2010) Switching of the core structures of glycosphingolipids from globo- and lacto- to ganglio-series upon human embryonic stem cell differentiation. *Proc Natl Acad Sci USA* 107(52):22564–22569.
27. Nguyen LV, Vanner R, Dirks P, Eaves CJ (2012) Cancer stem cells: An evolving concept. *Nat Rev Cancer* 12(2):133–143.
28. Bonnet D, Dick JE (1997) Human acute myeloid leukemia is organized as a hierarchy that originates from a primitive hematopoietic cell. *Nat Med* 3(7):730–737.
29. Uchida N, et al. (2000) Direct isolation of human central nervous system stem cells. *Proc Natl Acad Sci USA* 97(26):14720–14725.
30. Dalerba P, et al. (2007) Phenotypic characterization of human colorectal cancer stem cells. *Proc Natl Acad Sci USA* 104(24):10158–10163.
31. Al-Hajj M, Wicha MS, Benito-Hernandez A, Morrison SJ, Clarke MF (2003) Prospective identification of tumorigenic breast cancer cells. *Proc Natl Acad Sci USA* 100(7):3983–3988.
32. Terris B, Cavard C, Perret C (2010) EpCAM, a new marker for cancer stem cells in hepatocellular carcinoma. *J Hepatol* 52(2):280–281.
33. Dean M, Fojo T, Bates S (2005) Tumour stem cells and drug resistance. *Nat Rev Cancer* 5(4):275–284.
34. Creighton CJ, et al. (2009) Residual breast cancers after conventional therapy display mesenchymal as well as tumor-initiating features. *Proc Natl Acad Sci USA* 106(33):13820–13825.
35. Li X, et al. (2008) Intrinsic resistance of tumorigenic breast cancer cells to chemotherapy. *J Natl Cancer Inst* 100(9):672–679.
36. Phillips TM, McBride WH, Pajonk F (2006) The response of CD24(-/low)/CD44+ breast cancer-initiating cells to radiation. *J Natl Cancer Inst* 98(24):1777–1785.
37. Zhang M, Atkinson RL, Rosen JM (2010) Selective targeting of radiation-resistant tumor-initiating cells. *Proc Natl Acad Sci USA* 107(8):3522–3527.
38. Ponti D, et al. (2005) Isolation and in vitro propagation of tumorigenic breast cancer cells with stem/progenitor cell properties. *Cancer Res* 65(13):5506–5511.
39. Sheridan C, et al. (2006) CD44+/CD24- breast cancer cells exhibit enhanced invasive properties: an early step necessary for metastasis. *Breast Cancer Res* 8(5):R59.
40. Ricardo S, et al. (2011) Breast cancer stem cell markers CD44, CD24 and ALDH1: Expression distribution within intrinsic molecular subtype. *J Clin Pathol* 64(11):937–946.
41. Johnston MD, Maini PK, Jonathan Chapman S, Edwards CM, Bodmer WF (2010) On the proportion of cancer stem cells in a tumour. *J Theor Biol* 266(4):708–711.
42. Nieto MA (2009) Epithelial-mesenchymal transitions in development and disease: Old views and new perspectives. *Int J Dev Biol* 53(8-10):1541–1547.
43. Acloque H, Adams MS, Fishwick K, Bronner-Fraser M, Nieto MA (2009) Epithelial-mesenchymal transitions: The importance of changing cell state in development and disease. *J Clin Invest* 119(6):1438–1449.
44. Mani SA, et al. (2008) The epithelial-mesenchymal transition generates cells with properties of stem cells. *Cell* 133(4):704–715.
45. Morel AP, et al. (2008) Generation of breast cancer stem cells through epithelial-mesenchymal transition. *PLoS ONE* 3(8):e2888.
46. Yeung TM, Gandhi SC, Wilding JL, Muschel R, Bodmer WF (2010) Cancer stem cells from colorectal cancer-derived cell lines. *Proc Natl Acad Sci USA* 107(8):3722–3727.
47. Lapidot T, et al. (1994) A cell initiating human acute myeloid leukaemia after transplantation into SCID mice. *Nature* 367(6464):645–648.
48. Dick JE (2003) Breast cancer stem cells revealed. *Proc Natl Acad Sci USA* 100(7):3547–3549.
49. Elenbaas B, et al. (2001) Human breast cancer cells generated by oncogenic transformation of primary mammary epithelial cells. *Genes Dev* 15(1):50–65.
50. Sun H, et al. (2013) CD44(+)/CD24 (-) breast cancer cells isolated from MCF-7 cultures exhibit enhanced angiogenic properties. *Clin Transl Oncol* 15(1):46–54.
51. Cariati M, et al. (2008) Alpha-6 integrin is necessary for the tumourigenicity of a stem cell-like subpopulation within the MCF7 breast cancer cell line. *Int J Cancer* 122(2):298–304.
52. Dontu G, et al. (2003) In vitro propagation and transcriptional profiling of human mammary stem/progenitor cells. *Genes Dev* 17(10):1253–1270.
53. Charafe-Jauffret E, et al. (2009) Breast cancer cell lines contain functional cancer stem cells with metastatic capacity and a distinct molecular signature. *Cancer Res* 69(4):1302–1313.
54. Yamaji T, Nishikawa K, Hanada K (2010) Transmembrane BAX inhibitor motif containing (TMBIM) family proteins perturbs a trans-Golgi network enzyme, Gb3 synthase, and reduces Gb3 biosynthesis. *J Biol Chem* 285(46):35505–35518.
55. Schmitt F, Ricardo S, Vieira AF, Dionísio MR, Paredes J (2012) Cancer stem cell markers in breast neoplasias: Their relevance and distribution in distinct molecular subtypes. *Virchows Arch* 460(6):545–553.
56. Battula VL, et al. (2012) Ganglioside GD2 identifies breast cancer stem cells and promotes tumorigenesis. *J Clin Invest* 122(6):2066–2078.
57. Webb TJ, et al. (2012) Molecular identification of GD3 as a suppressor of the innate immune response in ovarian cancer. *Cancer Res* 72(15):3744–3752.
58. Becker R, Eichler MK, Jennemann R, Bertalanffy H (2002) Phase I clinical trial on adjuvant active immunotherapy of human gliomas with GD2-conjugate. *Br J Neurosurg* 16(3):269–275.
59. Shibuya H, et al. (2012) Enhancement of malignant properties of human osteosarcoma cells with disialyl gangliosides GD2/GD3. *Cancer Sci* 103(9):1656–1664.
60. Hakomori SI (1993) Structure and function of sphingoglycolipids in transmembrane signalling and cell-cell interactions. *Biochem Soc Trans* 21(3):583–595.
61. Scursoni AM, et al. (2011) Detection of N-glycolyl GM3 ganglioside in neuroectodermal tumors by immunohistochemistry: An attractive vaccine target for aggressive pediatric cancer. *Clin Dev Immunol* 2011:245181.
62. Chantada GL, et al. (2006) An aggressive bone marrow evaluation including immunocytology with GD2 for advanced retinoblastoma. *J Pediatr Hematol Oncol* 28(6):369–373.
63. Masamune H, Yosizawa Z, Oh-Uti K, Matuda Y, Masudawa A (1952) Biochemical studies on carbohydrates. CLVI. On the sugar components of the hexosamine-containing carbohydrates from gastric cancers, normal human gastric mucosa and human liver and of the glacial acetic acid-soluble proteins from those tissues as well as a metastasis in liver of gastric cancer. *Tohoku J Exp Med* 56(1–2):37–42.
64. Dahr W, Uhlenbruck G, Bird GWG (1974) Cryptic A-like receptor sites in human erythrocyte glycoproteins: proposed nature of Tn-antigen. *Vox Sang* 27(1):29–42.
65. Hirohashi S, Clausen H, Yamada T, Shimosato Y, Hakomori SI (1985) Blood group A cross-reacting epitope defined by monoclonal antibodies NCC-LU-35 and -81 expressed in cancer of blood group O or B individuals: Its identification as Tn antigen. *Proc Natl Acad Sci USA* 82(20):7039–7043.
66. Kjeldsen TB, et al. (1988) Preparation and characterization of monoclonal antibodies directed to the tumor-associated O-linked associated O-linked sialosyl-2–6 alpha-N-acetylgalactosaminyl (sialosyl-Tn) epitope. *Cancer Res* 48:2214–2220.
67. Watanabe M, et al. (1991) *In vitro* and *in vivo* antitumor effects of murine monoclonal antibody NCC-ST-421 reacting with dimeric $Le^{(a)}$ ($Le^{(a)}$/$Le^{(a)}$) epitope. *Cancer Res* 51(8):2199–2204.
68. Ito H, et al. (1992) Specificity and immunobiological properties of monoclonal antibody IMH2, established after immunization with $Le^{(b)}$/$Le^{(a)}$ glycosphingolipid, a novel extended type 1 chain antigen. *Cancer Res* 52(13):3739–3745.
69. Stroud MR, Levery SB, Salyan MEK, Roberts CE, Hakomori SI (1992) Extended type-1 chain glycosphingolipid antigens. Isolation and characterization of trifucosyl-Leb antigen (III4V4VI2Fuc3Lc6). *Eur J Biochem* 203(3):577–586.